

# An Investigation of the Synthesis of the Layered Perovskite $\text{RbCa}_2\text{Nb}_3\text{O}_{10}$ Using Time-Resolved *in Situ* High-Temperature Powder X-ray Diffraction

Margret J. Geselbracht,<sup>†</sup> Richard I. Walton,<sup>‡</sup> E. Sarah Cowell,  
Franck Millange, and Dermot O'Hare\*

Inorganic Chemistry Laboratory, South Parks Road, Oxford, OX1 3QR United Kingdom

Received May 13, 2002. Revised Manuscript Received July 25, 2002

The Dion–Jacobson-type layered perovskite,  $\text{RbCa}_2\text{Nb}_3\text{O}_{10}$ , has been prepared by two different synthetic routes at the moderate temperature of 800 °C. With a new molten salt approach, combining a 1:4:3 molar ratio of  $\text{K}_2\text{CO}_3:\text{CaCO}_3:\text{Nb}_2\text{O}_5$  with a large excess of  $\text{RbCl}$  leads to the rapid formation of  $\text{RbCa}_2\text{Nb}_3\text{O}_{10}$  at 800 °C. Although the product incorporates rubidium from the molten salt flux,  $\text{K}_2\text{CO}_3$  is a necessary component of the reaction mixture. Surprisingly, the solid-state reaction of a 1.5:4:3 molar ratio of  $\text{Rb}_2\text{CO}_3:\text{CaCO}_3:\text{Nb}_2\text{O}_5$  at 800 °C also leads to the formation of  $\text{RbCa}_2\text{Nb}_3\text{O}_{10}$  in a relatively short time. Both of these reactions were studied by time-resolved *in situ* high-temperature X-ray powder diffraction. Energy-dispersive X-ray diffraction (EDXRD) data confirmed that the synthesis of  $\text{RbCa}_2\text{Nb}_3\text{O}_{10}$  was accelerated by the molten salt flux; the material crystallizes as soon as the  $\text{RbCl}$  flux melts, and the reaction is shown to be complete within a few minutes of reaching 800 °C. The solid-state reaction proceeds more slowly but is still essentially complete in about 80 min. The *in situ* EDXRD data also revealed the presence of two or more intermediate phases produced in the solid-state synthesis, corroborated by laboratory quenching studies. Conventional high-temperature diffraction studies of  $\text{RbCa}_2\text{Nb}_3\text{O}_{10}$  established that no phase changes occur in this material up to 1000 °C.

## Introduction

A traditional synthetic tool of the solid-state chemist has been the high-temperature solid–solid reaction. The trademark high temperatures of this method (typically >800 °C) are required to overcome the very small diffusion rates of solid-state reactants. These high temperatures and the large furnaces they necessitate make it difficult to monitor physical and chemical changes taking place while the reaction occurs and thus to obtain information about the reaction mechanism and kinetics. One method of lowering the reaction temperatures and/or shortening reaction times for the synthesis of inorganic solids is the use of a molten salt flux. Although there are many examples in the literature of the use of molten salt fluxes to enhance reactivity and promote crystal growth,<sup>1</sup> little information is known about the mechanisms of these reactions or the intermediates produced. A notable exception was the report in 1995 on the probable mechanism for the molten salt synthesis of the commercially important X-ray phosphors,  $\text{M}'-\text{RTaO}_4$  ( $\text{R} = \text{Y, Gd, Lu}$ ), from  $\text{R}_2\text{O}_3$  and  $\text{Ta}_2\text{O}_5$ .<sup>2</sup> On the basis of thermal analysis data and X-ray

diffraction evidence for reaction intermediates isolated by quenching, Hedden et al. concluded that the molten salt flux reacted with the constituent oxides to form intermediates that are more reactive than the starting oxides, accelerating product formation and ultimately regenerating the flux. These detailed studies are rare, however, and as in the case of solid-state reactions, little is generally known about the kinetics or mechanisms of molten salt flux reactions.

One of us recently reported the use of a molten  $\text{KCl}$  flux to considerably lower the reaction temperature in the synthesis of the layered perovskite  $\text{KCa}_2\text{Nb}_3\text{O}_{10}$ .<sup>3</sup> Layered perovskites have attracted considerable attention recently because of their rich interlayer chemistry,<sup>4</sup> their use as photocatalysts,<sup>5</sup> their use as precursors to

(2) Hedden, D. B.; Torardi, C. C.; Zegarski, W. *J. Solid State Chem.* **1995**, *118*, 419.

(3) Geselbracht, M. J.; Scarola, R. J.; Ingram, D.; Green, C.; Caldwell, J. H. In *Solid State Chemistry of Inorganic Materials*; Davies, P. K., Jacobson, A. J., Torardi, C. C., Vanderah, T. A., Eds.; MRS Symposium Proceedings 453; Materials Research Society: Pittsburgh, PA, 1997; pp 147–152.

(4) (a) Jacobson, A. J. Synthesis and Reaction Chemistry of Layered Oxides with Perovskite Related Structures. In *Chemical Physics of Intercalation II*; Bernier, P., Fischer, J. E., Roth, S., Solin, S., Eds.; NATO ASI Series B, 305; Plenum Press: New York, 1993; pp 117–139. (b) Takahashi, S.; Nakato, T.; Hayashi, S.; Sugahara, Y.; Kuroda, K. *Inorg. Chem.* **1995**, *34*, 5065. (c) Mohan Ram, R. A.; Clearfield, A. *J. Solid State Chem.* **1995**, *112*, 288.

(5) (a) Takata, T.; Furumi, Y.; Shinohara, K.; Tanaka, A.; Hara, M.; Kondo, J. N.; Domen, K. *Chem. Mater.* **1997**, *9*, 1063. (b) Domen, K.; Ebina, Y.; Ikeda, S.; Tanaka, A.; Kondo, J. N.; Maruya, K. *Catal. Today* **1996**, *28*, 167. (c) Ebina, Y.; Tanaka, A.; Kondo, J. N.; Domen, K. *Chem. Mater.* **1996**, *8*, 2534. (d) Yoshimura, J.; Ebina, Y.; Kondo, J.; Domen, K.; Tanaka, A. *J. Phys. Chem.* **1993**, *97*, 1970.

\* To whom correspondence should be addressed.

† Permanent address: Reed College, 3203 SE Woodstock Blvd, Portland, OR 97202.

‡ Present address: School of Chemistry, University of Exeter, Stocker Road, Exeter, EX4 4QD U.K.

(1) See for example (a) Brahmarrout, B.; Messing, G. L.; Trolier-McKinstry, S. *J. Am. Ceram. Soc.* **1999**, *82*, 1565. (b) Gopalan, S.; Mehta, K.; Virkar, A. V. *J. Mater. Res.* **1996**, *11*, 1863. (c) Yoon, K. H.; Cho, Y. S.; Kang, D. H. *J. Mater. Res.* **1998**, *33*, 2977. (d) Arendt, R. H. *J. Electrochem. Soc.* **1987**, *134*, 733.

new materials<sup>6</sup> and thin films,<sup>7</sup> and the discovery of colossal magnetoresistance in layered perovskite manganates.<sup>8</sup> There have been several reports of the use of molten salt fluxes to grow crystals of layered perovskites, typically at high temperature. For example, crystals of  $\text{RbCa}_2\text{Nb}_3\text{O}_{10}$  were grown from a rubidium sulfate flux at 1300 °C.<sup>9</sup> We found that polycrystalline  $\text{RbCa}_2\text{Nb}_3\text{O}_{10}$  could be readily synthesized in a  $\text{RbCl}$  flux ( $\text{mp} = 718$  °C) at 800 °C. To gain some understanding of the chemical processes taking place during these molten salt reactions, we have investigated fully the synthesis of  $\text{RbCa}_2\text{Nb}_3\text{O}_{10}$  from molten  $\text{RbCl}$  fluxes and performed time-resolved *in situ* X-ray diffraction studies of both the molten salt synthesis and the solid-state synthesis of  $\text{RbCa}_2\text{Nb}_3\text{O}_{10}$  at 800 °C.

Developments in *in situ* powder X-ray diffraction over the past few years have largely been due to the availability of high-flux synchrotron X-ray sources that allow rapid data collection and that take advantage of the intense X-ray beams to penetrate bulky reaction containers.<sup>10</sup> Examples of the use of *in situ* X-ray diffraction to follow solid–solid reactions are the work of Bondioli et al., who tracked the reaction between  $\text{BaCO}_3$  and  $\text{TiO}_2$  in the laboratory and observed the formation of  $\text{Ba}_2\text{TiO}_4$  as an intermediate,<sup>11</sup> and a study of high temperature, self-propagating reactions by Larson et al., which revealed the presence of transient phases during the production of transition-metal carbides from the elements.<sup>12</sup> These studies both illustrate how the occurrence of intermediate crystalline phases can be observed by *in situ* X-ray diffraction. This information, in addition to the observation of the kinetics of the reaction, allows a reaction mechanism to be proposed. In most *in situ* X-ray diffraction experiments previously reported, the amount of sample studied must be very small to minimize absorption of the beam (both by the sample and by the reaction chamber) so that high-quality data may be collected in the shortest possible period of time. To reproduce more accurately real reaction conditions, we recently described the construction of a large-volume furnace, from which energy-dispersive X-ray diffraction (EDXRD) data can be measured during chemical reactions taking place at temperatures up to 1000 °C.<sup>13</sup> In this paper we describe the first application of the apparatus and, to the best of our knowledge, the first *in situ* diffraction study of a molten salt synthesis, namely, the formation of  $\text{RbCa}_2\text{Nb}_3\text{O}_{10}$ .

(6) (a) Schaak, R. E.; Mallouk, T. E. *J. Am. Chem. Soc.* **2000**, *122*, 2798. (b) Gopalakrishnan, J.; Sivakumar, T.; Ramesha, K.; Thangadurai, V.; Subbanna, G. N. *J. Am. Chem. Soc.* **2000**, *122*, 6237. (c) Kodenkandath, T. A.; Kumbhar, A. S.; Zhou, W. L.; Wiley, J. B. *Inorg. Chem.* **2001**, *40*, 710. (d) Schaak, R. E.; Mallouk, T. E. *Chem. Mater.* **2002**, *14*, 1455.

(7) Schaak, R. E.; Mallouk, T. E. *Chem. Mater.* **2000**, *12*, 2513.

(8) (a) Moritomo, Y.; Asamitsu, A.; Kuwahara, H.; Tokura, Y. *Nature* **1996**, *380*, 141. (b) Battle, P. D.; Green, M. A.; Laskey, N. S.; Millburn, J. E.; Rosseinsky, M. J.; Sullivan, S. P.; Vente, J. F. *Chem. Commun.* **1996**, 767.

(9) Dion, M.; Ganne, M.; Tournoux, M. *Rev. Chim. Miner.* **1986**, *23*, 61.

(10) Walton, R. I.; O'Hare, D. *Chem. Commun.* **2000**, 2283.

(11) Bondioli, K.; Bonamartini-Corradi, A.; Ferrari, A. M.; Manfredini, T.; Pellacani, G. C. *Mater. Sci. Forum* **1998**, *278–281*, 379.

(12) Larson, E. M.; Wong, J.; Holt, J. B.; Waide, P. A.; Nutt, G.; Rupp, B.; Terminello, L. J. *J. Mater. Res.* **1993**, *8*, 1533.

(13) Geselbracht, M. J.; Walton, R. I.; Cowell, E. S.; Millange, F.; O'Hare, D. *Rev. Sci. Instrum.* **2000**, *71*, 4177.

## Experimental Section

All starting materials were obtained from commercial suppliers. Metal carbonates and metal chlorides were typically dried overnight at 120 °C prior to use. Molten salt reactions were carried out either in alumina boats or in fused silica tubes, open to the atmosphere. After a reaction, the molten salt flux was dissolved in deionized water and insoluble products were isolated for characterization by X-ray powder diffraction.

**Laboratory Studies.** Conventional X-ray diffraction patterns were recorded at room temperature on a Phillips PW 1729 diffractometer, using  $\text{Cu K}\alpha$  radiation. High-temperature X-ray diffraction data were recorded in the laboratory under a flow of He gas on a Siemens D5000 diffractometer with an HTK1200 Anton-Parr cell from 3° to 90°  $2\theta$  with a step size of 0.02° and count time of 2 s/step. Diffraction patterns were obtained at 28, 800, 900, 1000, and 28 °C, again after cooling from high temperature from  $\text{RbCa}_2\text{Nb}_3\text{O}_{10}$  to confirm that no structural transition takes place at the temperatures used in the synthesis.

**In Situ EDXRD Data.** *In situ* EDXRD experiments were performed on Station 16.4 of the Synchrotron Radiation Facility (SRS), Daresbury Laboratory, U.K. This second generation synchrotron source operates with an average stored current of 200 mA and a typical beam energy of 2 GeV. Station 16.4 is illuminated with radiation from a 6 T superconducting wiggler and receives X-rays over an energy range of 5–120 keV with a maximum X-ray flux of  $3 \times 10^{10}$  photons/s at around 13 keV. The position of this energy maximum is shifted by the absorption of lower energy photons by the sample containers so that, in practice, X-rays with energies above ~30 keV are useful. Data were measured from reactions taking place in fused silica tubes (9 × 12 mm, i.d. × o.d.) held in a vertical tube furnace, the design, construction, and calibration of which we have previously described in detail.<sup>13</sup> The EDXRD method allows rapid data collection since the incident X-ray flux is high, and all diffraction data are measured simultaneously by a fixed-angle, solid-state detector. In the EDXRD experiment, Bragg reflections with an interplanar spacing [ $d$  (Å)] are characterized by an energy [ $E$  (keV)], given by

$$E = 6.19926/(d \sin \theta) \quad (1)$$

where  $2\theta$  is the angle of the detector relative to the incident beam.<sup>14</sup> Station 16.4 is equipped with a novel three-element detector,<sup>15</sup> and this allows three regions of diffraction data to be recorded, and therefore unambiguous identification of crystalline phases.<sup>16</sup> Bragg reflections of crystalline standard materials were used to determine accurately the angle of each detector element (silicon for the higher angle detectors and zeolite A for the low-angle detector); the top detector was set at  $2\theta = 7.47^\circ$ , the middle at  $2\theta = 4.63^\circ$ , and the bottom at  $2\theta = 1.83^\circ$ . Data were collected in periods of 60–120 s (see below) from both molten salt and solid–solid reactions taking place within the furnace. After completion of *in situ* studies, all reaction products were analyzed by powder X-ray diffraction collected at room temperature on a laboratory diffractometer to check sample purity. Data analysis was performed using the freely available programs DLConvert and XFIT;<sup>17</sup> this allowed conversion of the data into ASCII format, plotting of data from individual runs and the determination of peak areas.

## Results and Discussion

### 1. Laboratory Studies of the Synthesis of $\text{RbCa}_2\text{Nb}_3\text{O}_{10}$ . Reaction of $\text{K}_2\text{CO}_3$ , $\text{CaCO}_3$ , and $\text{Nb}_2\text{O}_5$ in a 1:4:3

(14) Giessen, B. C.; Gordan, G. E. *Science* **1968**, *159*, 973.

(15) Colston, S. L.; Jacques, S. D. M.; Barnes, P.; Jupe, A. C.; Hall, C. J. *Synchrotron Radiat.* **1998**, *5*, 310.

(16) Muncaster, G.; Davies, A. T.; Sankar, G.; Catlow, C. R. A.; Thomas, J. M.; Colston, S. L.; Barnes, P.; Walton, R. I.; O'Hare, D. *Phys. Chem. Chem. Phys.* **2000**, *2*, 3523.

(17) Software available from <http://www.ccp14.ac.uk>, 2002.

molar ratio together with a large excess of  $\text{RbCl}$  readily produced the layered perovskite  $\text{RbCa}_2\text{Nb}_3\text{O}_{10}$  at 800 °C. The reaction incorporated rubidium from the flux to form the rubidium layered perovskite rather than the intended potassium analogue. Initial laboratory studies indicated that the product formed in under an hour and that reaction times ranging from 1 to 24 h resulted in little difference in the product. Although the alkali metal in the product clearly came from the flux,  $\text{K}_2\text{CO}_3$  was a necessary component in the reaction as heating  $\text{CaCO}_3$  and  $\text{Nb}_2\text{O}_5$  in a 4:3 molar ratio together with a large excess of  $\text{RbCl}$  at 800 °C produced only calcium niobates,  $\text{CaNb}_2\text{O}_6$  and  $\text{Ca}_2\text{Nb}_2\text{O}_7$ . Interestingly, heating the potassium layered perovskite,  $\text{KCa}_2\text{Nb}_3\text{O}_{10}$ , in molten  $\text{RbCl}$  at 800 °C for 24 h led to the ion-exchange product  $\text{RbCa}_2\text{Nb}_3\text{O}_{10}$ . This result suggests that one possible explanation for needing  $\text{K}_2\text{CO}_3$  in the reaction mixture is that the reaction takes place via a  $\text{KCa}_2\text{Nb}_3\text{O}_{10}$  intermediate. Alternatively, the potassium in  $\text{K}_2\text{CO}_3$  may not be the important factor at all but rather the  $\text{K}_2\text{CO}_3$  decomposition is crucial for maintaining a critical oxide ion concentration in the flux.

The effect of reagent concentration in the flux was investigated by varying the  $\text{K}_2\text{CO}_3:\text{CaCO}_3:\text{Nb}_2\text{O}_5:\text{RbCl}$  molar ratios from 1:4:3:100 to 1:4:3:50 to 1:4:3:20 to 1:4:3:2. As long as a large molar excess of  $\text{RbCl}$  was present (1:4:3:100 or 1:4:3:50 molar ratios), single-phase  $\text{RbCa}_2\text{Nb}_3\text{O}_{10}$  was obtained. However, when the reagent/salt ratio dropped to 1:4:3:20 or 1:4:3:2, increasing amounts of impurity phases were observed in the X-ray powder diffraction patterns of the products. In the product from the 1:4:3:20 reaction, trace amounts of  $\text{CaNb}_2\text{O}_6$  can be identified, and in the product from the 1:4:3:2 reaction,  $\text{CaNb}_2\text{O}_6$  is present in larger quantities together with  $\text{Ca}_2\text{Nb}_2\text{O}_7$ . Clearly, the optimal conditions involve a large excess of  $\text{RbCl}$ . The rapid formation of  $\text{RbCa}_2\text{Nb}_3\text{O}_{10}$  in the  $\text{RbCl}$  flux at 800 °C prompted us to investigate the traditional solid-state synthesis at the same temperature. The original preparation of  $\text{RbCa}_2\text{Nb}_3\text{O}_{10}$  reported in the literature involved firing a mixture of  $\text{Rb}_2\text{SO}_4$ ,  $\text{Ca}_2\text{Nb}_2\text{O}_7$ , and  $\text{Nb}_2\text{O}_5$ , first at 750 °C and then at 1250 °C over the course of 2 days.<sup>18</sup> We found, however, that simply heating  $\text{Rb}_2\text{CO}_3$ ,  $\text{CaCO}_3$ , and  $\text{Nb}_2\text{O}_5$  in a 1.5:4:3 molar ratio (50% molar excess  $\text{Rb}_2\text{CO}_3$ ) at 800 °C for 24 h produced single-phase  $\text{RbCa}_2\text{Nb}_3\text{O}_{10}$ .

Before the in situ experiments were undertaken, high-temperature X-ray powder diffraction data were collected from  $\text{RbCa}_2\text{Nb}_3\text{O}_{10}$  using a laboratory diffractometer to verify that no phase transitions occurred up to 800 °C. Data were collected at 28, 800, and 1000 °C and again at 28 °C after cooling from high temperature. Aside from the expected thermal expansion at high temperatures, no significant changes were observed in the X-ray diffraction patterns. Lattice parameters for  $\text{RbCa}_2\text{Nb}_3\text{O}_{10}$  refined from the peak positions of 17–20 reflections at each temperature are collected in Table 1. No phase transitions were observed in this sample up to 1000 °C. The diffraction data at 800 °C were subsequently used to confirm assignment of the product peaks in the in situ EDXRD patterns obtained during the synthesis of  $\text{RbCa}_2\text{Nb}_3\text{O}_{10}$  (see below).

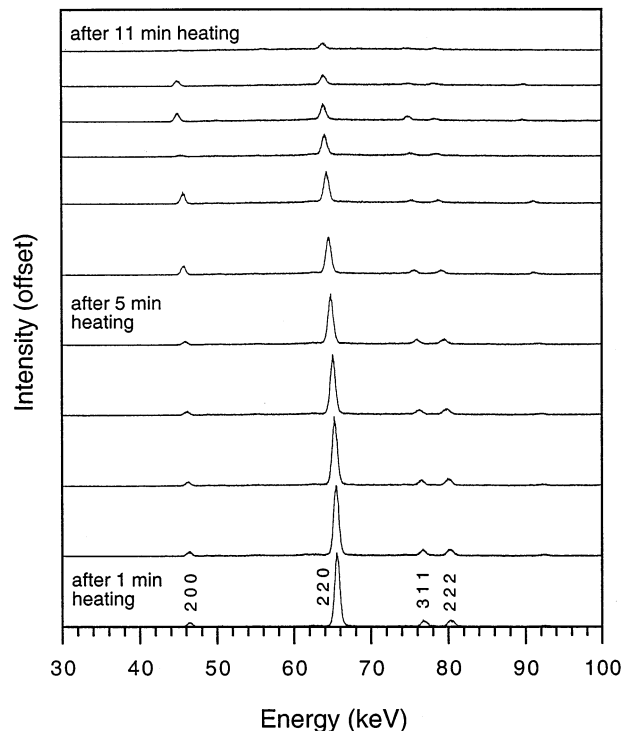


**Figure 1.** In situ EDXRD data from the middle detector ( $2\theta = 4.63^\circ$ ) collected every minute from a molten  $\text{RbCl}$  flux synthesis as the furnace is heated to 800 °C. All of the peaks are due to crystalline  $\text{RbCl}$  and shift to lower energies (higher  $d$  spacings) as the furnace is heated, consistent with thermal expansion. Peak intensities decrease until finally the  $\text{RbCl}$  melts.

**Table 1. Tetragonal Lattice Parameters for  $\text{RbCa}_2\text{Nb}_3\text{O}_{10}$  Refined from X-ray Powder Diffraction Data Collected in the Laboratory at Several Temperatures**

temp (°C)	$a$ (Å)	$c$ (Å)	volume (Å $^3$ )
28	7.720(1)	14.909(3)	888.6(2)
800	7.776(1)	15.138(4)	915.3(3)
1000	7.787(1)	15.206(3)	922.1(3)
28 (postheating)	7.718(1)	14.914(2)	888.4(2)
literature <sup>18</sup>	7.725(2)	14.909(5)	889.7

**2. In Situ EDXRD Data. Molten Salt Synthesis of  $\text{RbCa}_2\text{Nb}_3\text{O}_{10}$ .** Figure 1 shows EDXRD data measured by the middle detector every 60 s during the early stages of heating a 1:4:3:50 molar ratio of the reactants  $\text{K}_2\text{CO}_3:\text{CaCO}_3:\text{Nb}_2\text{O}_5:\text{RbCl}$  to 800 °C. The furnace takes a short period of time to reach the desired temperature, so the early data are dominated by the Bragg reflections of  $\text{RbCl}$ . As the temperature rises, we observe the thermal expansion and melting of  $\text{RbCl}$  evidenced by the shift of these reflections to lower energies (higher  $d$  spacings) and, ultimately, the disappearance of these peaks. The positions of the four peaks labeled in Figure 1 were determined for the first 10 spectra using the peak-fitting routine XFIT, and the  $d$  spacings were used to refine a set of unit cell parameters. Figure 2a shows a plot of the refined cell parameters of  $\text{RbCl}$  as a function of time. By comparison of these data with the literature values for the cell parameter of  $\text{RbCl}$  as a function of temperature,<sup>19</sup> we can calculate a temperature curve for the sample as a function of time, shown in Figure 2b. It should be pointed out that the melting

(18) Dion, M.; Ganne, M.; Tournoux, M. *Mater. Res. Bull.* **1981**, 16, 1429.

(19) Srivastava, K. K.; Merchant, H. D. *J. Phys. Chem. Solids* **1973**, 34, 2069.

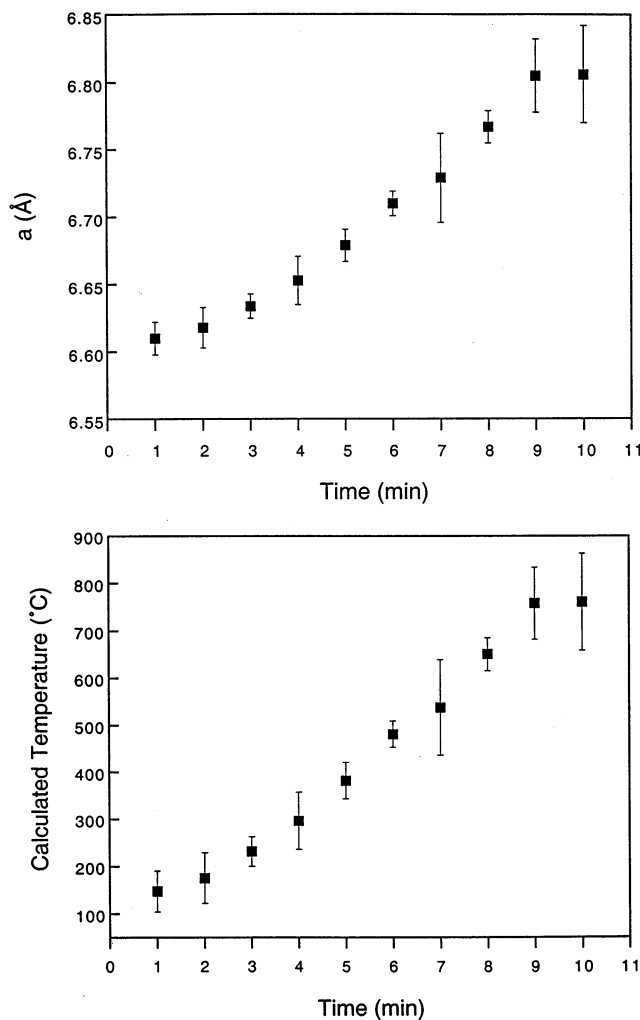


**Figure 2.** (a) Variation in the cubic cell parameter for RbCl as a function of furnace heating time (top). Cell parameters were refined from the peak positions of the EDXRD data shown in Figure 1. Error bars were generated by assuming a deviation of  $\pm 3\sigma$  from the refined lattice parameter. (b) With use of published thermal expansion data for RbCl, the temperature of the sample at each point in time was calculated from the cell parameter (bottom). The maximum deviations of the lattice parameter at each point were used to estimate the errors in the calculated temperatures. These data show that the furnace heats to 800 °C rapidly, within the first 12 min of heating.

point of RbCl is 718 °C. The last two data points in Figure 2b lie above this value, although the error bars on these temperatures are also quite large and fully encompass the melting point temperature. The data in Figures 1 and 2 demonstrate that the desired reaction temperature (800 °C) is achieved within the first 12 min just as the RbCl salt melts.

Figure 3a shows EDXRD data measured on this same reaction mixture just before and after the melting of RbCl. Three Bragg reflections of the product RbCa<sub>2</sub>Nb<sub>3</sub>O<sub>10</sub> are seen immediately after the salt melts; these do not increase in intensity after 13 min of reaction time. We attempted to study this molten salt synthesis at a lower temperature to observe the growth of product over a longer time scale. Figure 3b shows the data obtained from an identical reaction heated to 750 °C. Once again the product appears immediately after the melting of the salt mixture, and in this case after 16 min, the

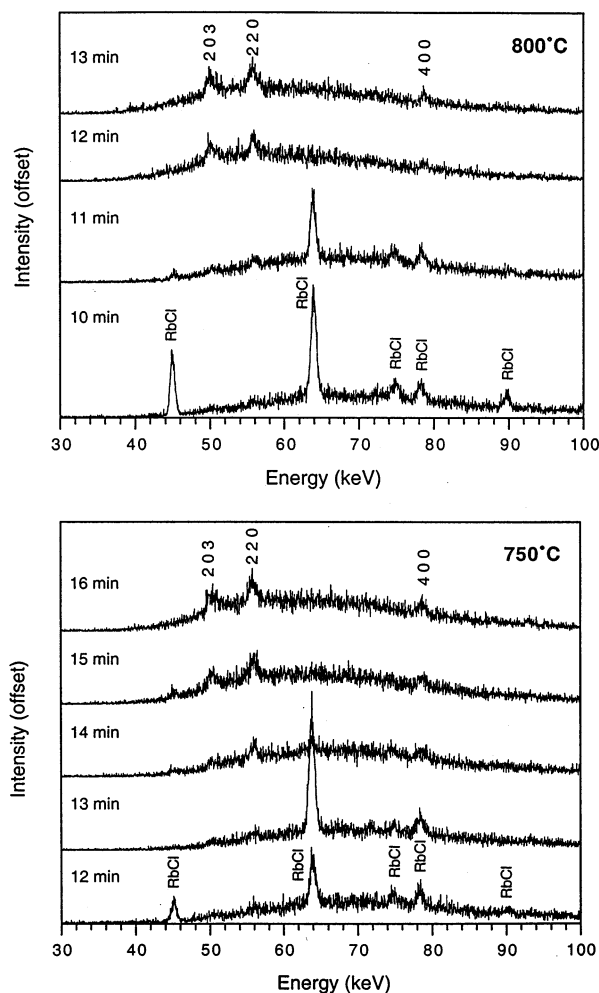


**Figure 3.** Selected in situ EDXRD data from the middle detector ( $2\theta = 4.63^\circ$ ) for molten RbCl flux syntheses carried out at (a) 800 °C (top) and (b) 750 °C (bottom). In both cases, weak peaks from RbCa<sub>2</sub>Nb<sub>3</sub>O<sub>10</sub>, identified with the Miller indices 203, 220, and 400 from a tetragonal unit cell, are discernible as the salt begins to melt.

reaction is complete. Although we have observed for the first time the rapidity of the molten salt reaction, we were unable to extract accurate peak areas to determine crystallization curves. The rapid growth in peak intensity (the reaction was complete after acquisition of only 2–3 spectra) and the high background noise of the data made peak area determination difficult. The background in the data is presumably due to a high level of absorption and amorphous scattering of the X-ray beam by the liquid RbCl flux. This would also explain why we were unable to observe any useable signal in the higher angle top detector after the RbCl melted; the scattered beam has to pass through a larger amount of sample before reaching the top detector. In other experiments we have performed involving molten salts with lighter atoms (NaCl/KCl mixtures, for example), the background scatter and absorption by the salt were far less problematic.<sup>20</sup>

On the basis of laboratory evidence for the necessity of K<sub>2</sub>CO<sub>3</sub> in the reaction mixture, we speculated earlier that the molten salt synthesis of RbCa<sub>2</sub>Nb<sub>3</sub>O<sub>10</sub> might

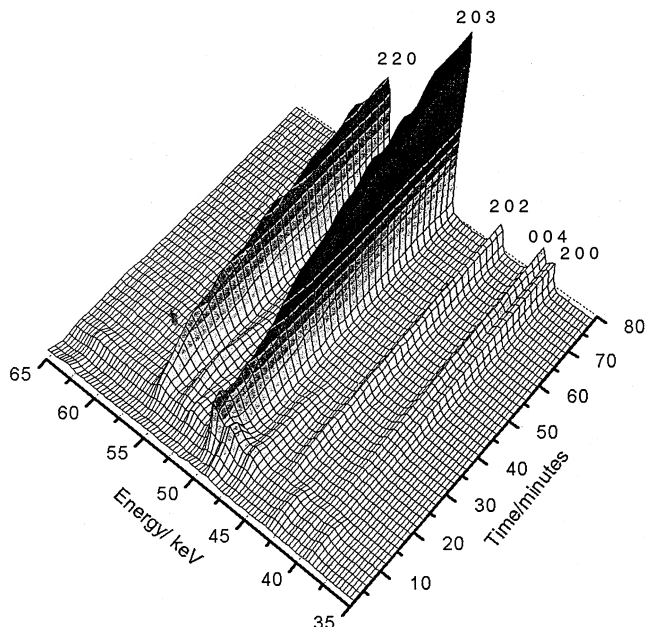
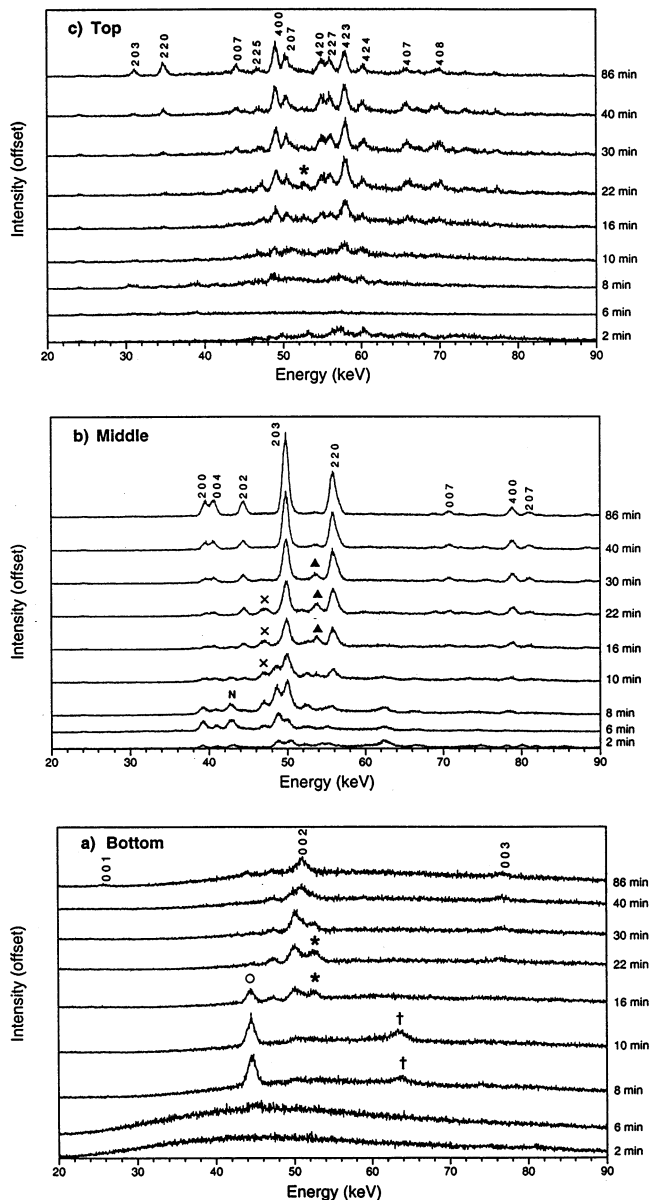


**Figure 4.** In situ EDXRD data from the middle detector ( $2\theta = 4.63^\circ$ ) for the solid-state synthesis of  $\text{RbCa}_2\text{Nb}_3\text{O}_{10}$  at  $800^\circ\text{C}$ . Bragg reflections for the product are labeled with  $hkl$ /Miller indices based on a tetragonal unit cell.

take place via a  $\text{KCa}_2\text{Nb}_3\text{O}_{10}$  intermediate. We can find no indication for the transient formation of  $\text{KCa}_2\text{Nb}_3\text{O}_{10}$  in the EDXRD data, although the speed of the reaction and the poor signal-to-noise of the data may be masking evidence for any intermediates.

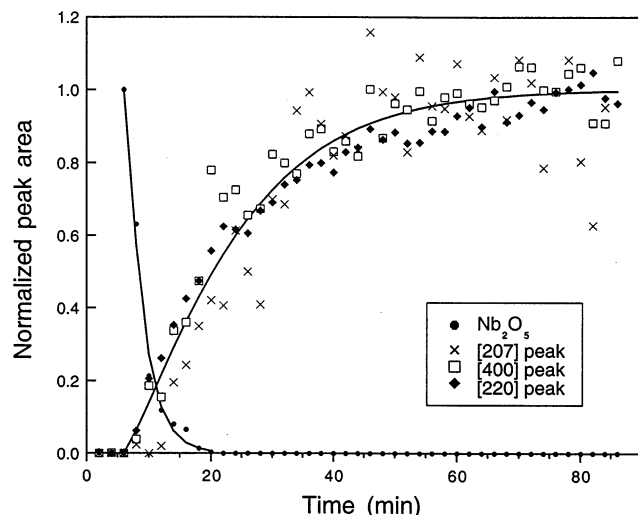
**Solid-State Synthesis of  $\text{RbCa}_2\text{Nb}_3\text{O}_{10}$ .** Figure 4 shows a three-dimensional stacked plot of EDXRD data measured every 120 s by the middle detector during the formation of  $\text{RbCa}_2\text{Nb}_3\text{O}_{10}$  from  $\text{Rb}_2\text{CO}_3$  (50% molar excess),  $\text{CaCO}_3$ , and  $\text{Nb}_2\text{O}_5$  at  $800^\circ\text{C}$ . The data allow us to make a number of observations: (i) there is a considerably reduced background in this reaction compared to the molten salt reaction, thus confirming our view that the presence of liquid-alkali-metal halide gives rise to significant background scatter and (ii) the solid-state reaction takes place on a longer time scale than the molten-salt reaction, making the process more amenable for study by our EDXRD cell. We can also see the presence of transient crystalline phases at the early stages of reaction. Two-dimensional plots of the data allow these transient phases to be identified more easily (Figure 5). In the data from the bottom detector (Figure 5a), we observe three distinct transient diffraction features. In the data from the middle detector (Figure 5b), we see the decay of  $\text{Nb}_2\text{O}_5$ , the presence of two intermediate phases, and the growth of the product. (Note that some of the peaks due to starting materials fluctuate in intensity during the first 6 min; this is most likely due to initial sample movement caused by the rapid heating.) In the data from the top detector (Figure 5c), the fluctuation of starting material peaks is again apparent, but after 6 min, when the material has resettled, product growth progresses smoothly. We also see one transient diffraction feature in the data from the top detector.

Figure 6 shows a decay curve for  $\text{Nb}_2\text{O}_5$  and growth curves for  $\text{RbCa}_2\text{Nb}_3\text{O}_{10}$  determined by integration of selected peaks from the data in Figure 5. For  $\text{Nb}_2\text{O}_5$ ,



**Figure 5.** In situ EDXRD data at selected times from the solid-state synthesis of  $\text{RbCa}_2\text{Nb}_3\text{O}_{10}$  at  $800^\circ\text{C}$ . (a) Data from the bottom detector ( $2\theta = 1.83^\circ$ ), where three intermediate peaks, each with a slightly different time profile, are marked with the symbols (○), (\*), and (†). (b) Data from the middle detector ( $2\theta = 4.63^\circ$ ), where one peak from the starting material  $\text{Nb}_2\text{O}_5$  is marked with N and two intermediate peaks are marked with symbols (x) and (▲). (c) Data from the top detector ( $2\theta = 7.47^\circ$ ), where the presence of a weak intermediate peak is indicated with an asterisk (\*). For all three detectors, peaks due to the product  $\text{RbCa}_2\text{Nb}_3\text{O}_{10}$  are labeled with  $hkl$  Miller indices based on a tetragonal unit cell.

we chose the well-resolved Bragg reflection at 42.9 keV ( $d = 3.57\text{ \AA}$ ) in the middle detector, and for  $\text{RbCa}_2\text{Nb}_3\text{O}_{10}$ , the 220 Bragg peak from the middle detector (55.8 keV,  $2.75\text{ \AA}$ ), and the 400 and 207 peaks from the top detector (49.0 keV,  $1.94\text{ \AA}$  and 50.1 keV,  $1.90\text{ \AA}$ , respectively). It proved impossible to obtain such curves for all Bragg peaks observed because first many overlap with each other, making partitioning of the area to individual peaks very difficult, and second at the beginning of the reaction many peaks overlap with those of the starting materials. The most striking feature of the product growth is that the curves obtained by



**Figure 6.** Normalized integrated peak areas for the decay of one  $\text{Nb}_2\text{O}_5$  starting material reflection compared to the growth of three different product peaks indexed to a tetragonal unit cell for  $\text{RbCa}_2\text{Nb}_3\text{O}_{10}$ . Curves are added as a visual guide only.

analysis of three different Bragg reflections are superimposable, even though they arise from Miller planes with different crystallographic orientations. This suggests that crystal growth is isotropic. Qualitative observations of the changing diffraction patterns in Figure 5 also provide evidence for this. For example, the closely spaced 200 and 004 reflections seen at  $\sim 40$  keV in the middle detector clearly grow at the same rate, even though at the early stages of reaction they overlap with peaks due to the starting materials. Thus, even though we are observing the growth of a layered perovskite material whose structure may be described as being highly anisotropic, there is no evidence for more rapid crystal growth in one particular crystallographic direction. A second important observation about these data is that a large amount of  $\text{Nb}_2\text{O}_5$  has been consumed before the  $\text{RbCa}_2\text{Nb}_3\text{O}_{10}$  crystallizes. The decay curve of the starting material and the growth curve of the product clearly do not cross at  $\alpha = 0.5$  ( $\alpha$  is the extent of reaction on a scale of 0–1). This suggests that the  $\text{Nb}_2\text{O}_5$  is converted into another phase (potentially an amorphous niobium oxide or a ternary or quaternary phase produced by reaction with the other components) before the onset of crystallization of the product. Our observation of intermediate crystalline phases is consistent with this idea.

Peak area analysis was also performed on several of the intermediate peaks seen during the reaction. In this case, difficulties were encountered when peaks overlapped with both product and starting material peaks, but it was possible to measure independently the areas of three of the transient peaks. The well-resolved intermediate peak in the bottom detector at 44.6 keV (8.75 Å), marked with an open circle in Figure 5a, was successfully integrated. From the middle detector, the intermediate peaks marked with  $\times$  and with filled triangles in Figure 5b (at 47.0 keV, 3.26 Å and 53.8 keV, 2.85 Å, respectively) were also integrated. The results of these analyses are shown in Figure 7. Given the different time profiles observed for these intermediate peaks, we conclude that there is more than one intermediate phase present.

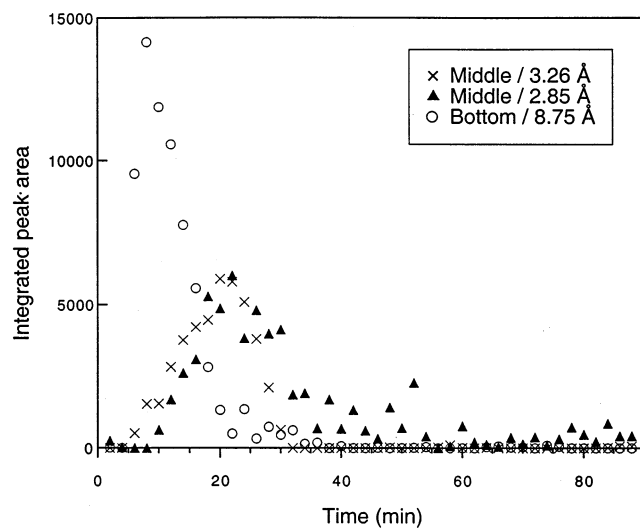


**Figure 7.** Integrated peak areas showing the growth and decay of three different intermediate peaks, two from the middle detector and one from the bottom detector. The symbols used in this plot match those used to mark these intermediate peaks in Figure 5a,b.

In an effort to identify the intermediate phases, several quenching studies were attempted back in the laboratory. The identical furnace and reaction conditions were used in these studies to mimic the environment of the in situ experiments in every respect. Samples of the solid-state reaction mixture were heated from room temperature to 800 °C and then quenched in air after a specified amount of time. In one case, the reaction was quenched after heating for 10 min, and in a second case, the reaction was quenched after heating for 20 min. These quenched samples were analyzed by X-ray diffraction on a laboratory diffractometer, taking advantage of the much higher resolution of Bragg reflections as compared to the EDXRD technique. In both quenched samples, the predominant crystalline phase isolated was the product  $\text{RbCa}_2\text{Nb}_3\text{O}_{10}$ , providing corroborative evidence for the rapidity of product growth. In addition to peaks due to  $\text{RbCa}_2\text{Nb}_3\text{O}_{10}$ , each of the quenched samples also contained smaller diffraction peaks due to other phases. The sample quenched after 10 min contained very small amounts of  $\text{Rb}_4\text{Nb}_6\text{O}_{17}$ , although none was present in the sample quenched after 20 min. There were a number of unidentified diffraction peaks observed in both quenched samples. It is interesting to note that three of these peaks index to a simple cubic unit cell with a lattice parameter (3.99 Å) similar to that of a perovskite-type structure. Given that the structure of  $\text{RbCa}_2\text{Nb}_3\text{O}_{10}$  is built from perovskite-type slabs, chemically, this would be a very plausible intermediate structure. There is some correlation between transient diffraction peaks observed in the in situ EDXRD data: specifically, peaks at 8.80, 3.28 and 3.20, and 2.82 Å observed in the quenched samples agree with the three EDXRD intermediate peaks whose temporal profiles are shown in Figure 7. No unambiguous assignment of these diffraction features was, however, possible. Further study of these samples by high-resolution electron microscopy and electron diffraction would be invaluable in the identification of these intermediate phases.

### Conclusions

The first time-resolved *in situ* X-ray powder diffraction studies of the high-temperature formation of the layered perovskite RbCa<sub>2</sub>Nb<sub>3</sub>O<sub>10</sub> has allowed insight into the complexities involved in its synthesis. A new molten salt route to the solid facilitates the rapid formation of RbCa<sub>2</sub>Nb<sub>3</sub>O<sub>10</sub>; we observed the crystallization of the material as soon as the RbCl flux melts, and the reaction is shown to be complete within a few minutes of reaching 800 °C. Although the data from this experiment are affected by strong background signal, the crystallization is obviously much more rapid than that in a traditional solid-state route, where the reaction takes around 80 min to reach completion. On the basis of the *in situ* EDXRD data and on laboratory quenching studies, the solid-state reaction appears to involve two or more intermediate phases. The data we have acquired are the first that will enable the pathways of

these complex reactions to be understood. Our results suggest that a detailed study of quenched materials will be a profitable line of future research. The application of this *in situ* X-ray diffraction technique to other high-temperature solid–solid and molten salt reactions will offer an unprecedented view into the possible mechanisms of these reactions and should advance our understanding of the processes used to make solid-state materials.

**Acknowledgment.** We thank the EPSRC for access to the Synchrotron Radiation Source (SRS), Daresbury Laboratory, and Dr. D. J. Taylor for his assistance with running the synchrotron experiments. M.J.G. thanks NSF (DMR-9733329) and the Michael E. Levine Faculty Research Fund, Reed College, for financial support.

CM020176V